Eur. J. Mech., A/Solids, **14,** n° 5, 721-745, 1995

Post-bifurcation and imperfection sensitivity of space trusses with many simultaneously buckling bars and a strongly nonlinear prebuckling solution

N. TRIANTAFYLLIDIS* and R. PEEK**

ABSTRACT. – Space trusses whose joints do not transmit moments enjoy a wide variety of engineering applications. These structures are usually highly symmetric and are made of large numbers of identical high strength but slender members. Due to the simultaneous buckling of their identical members, these structures have a multiple bifurcation point at their first buckling load, a situation that can lead to a strong imperfection sensitivity. A general finite displacement and rotation theory for elastic space trusses with out-of-straight deforming members, which has recently been proposed by the authors, is applied to structures with strongly nonlinear principal equilibrium paths. For small imperfection amplitudes, the imperfection sensitivity of these structures as well as the worst imperfection shape can be calculated from the bifurcated equilibrium branches for the perfect structure using an asymptotic method. The asymptotic results for the bifurcated equilibrium branches of the perfect structure are compared with the corresponding exact results in order to assess the validity of the proposed approach.

1. Introduction and motivation

Lattice-type truss structures are routinely used in many engineering applications. Examples include building roofs with large spans, crane booms, radio antennae and radio telescopes, just to name a few. Due to their high strength-to-weight ratio, lattice truss structures are also being envisioned for space applications such as solar panels, radio-astronomy dishes, communications platforms and space station structures (like the final design considered for the US Space Station Freedom). Due to the stringent weight considerations and the availability of high strength materials, the designs for large space structures lead to increasingly long and flexible members, a situation for which buckling becomes an important design consideration.

Frequently, the designs of these structures call for a high degree of geometric symmetry and involve large numbers of identical members. Depending also on the symmetry of the externally applied loading, a high number of members can simultaneously reach their lowest buckling load. For trusses, due to the inability of the joints to transmit moments,

* Department of Aerospace Engineering, The University of Michigan, Ann Arbor, MI 48109-2140, U.S.A.
** Department of Civil Engineering, The University of Michigan, Ann Arbor, MI 48109-2140, U.S.A.

EUROPEAN JOURNAL OF MECHANICS, A/SOLIDS, VOL. 14, N° 5, 1995
0997-7538/95/05/$ 4.00/© Gauthier-Villars

the buckling of each member corresponds to an eigenmode of the entire structure. Consequently, the space structures of interest can have multiple bifurcation points, *i.e.* critical points with a large number of corresponding simultaneous eigenmodes. Such structures can be extremely sensitive to the inevitable geometric, material and loading imperfections. The determination of the worst such possible imperfection shapes is thus a very important design issue.

The study of bifurcation and stability in structures with simultaneous or nearly simultaneous modes is a classical problem in solid mechanics. As such, it has received a great deal of attention in the engineering literature, especially after Koiter's [1945] pioneering work that put the problem on a sound mathematical basis. For the case of small imperfections, Koiter has also shown that the behavior of the imperfect structure can be deduced from the study of the perfect one. Consequenly the worst imperfection shape in a structure with simultaneous (or nearly simultaneous) modes can be found by analyzing the corresponding perfect structure (*see* Koiter [1976] for the worst imperfection shape result and also Triantafyllidis and Peek [1992] for a concise overview the corresponding general theory). The imperfection sensitivity of lattice structures has been discussed in several previous works (Wright [1965], Castaño [1989], Britvec [1973], Britvec & Davister [1985]). The simultaneous local buckling modes can coincide with a global buckling mode, thus aggravating the imperfection sensitivity of trusses, as for example in the case of lattice columns (*see* Thomphson & Hunt [1973], Byskov [1979], Crawford & Benton [1980], Elyada [1985]). A general theory addressing the imperfection sensitivity and the worst imperfection shape issues in arbitrary trusses has recently been presented by Peek and Triantafyllidis [1992]. The theory was used to study two and three dimensional truss structures, with essentially linear prebuckling configurations and under force control, for which the buckling of the individual members of the truss occurs prior to its first global buckling. The imperfection sensitivity results found were independent of the applied loading, except in the neighborhood of the loading corresponding to the first global bifurcation. On a subsequent paper, Peek [1993] has examined the interaction between the local (member buckling) and global (overall structural buckling) modes and found that the worst imperfection shape involves the interaction of the global mode with only one local mode.

The goal of the present paper is twofold: First to see the effect of a strongly nonlinear prebuckling solution on the imperfection sensitivity of space trusses. Second to assess the validity of the asymptotic expansions, used to calculate the bifurcated equilibrium paths near the critical load, by comparing them to the exact bifurcated equilibrium paths of the structure. The organization of this paper is as follows: Section 2 sets the governing equations for an arbitrary space truss with members that deform out-of-straight due to bending. The asymptotic analysis of the bifurcated equilibrium paths of the perfect solution, the discussion of their stability and the selection of the worst imperfection shape are presented in Section 3. The general analysis of the two previous sections is applied to two dome-like space trusses, under nodal forces perpendicular to the basis plane, both of which exhibit a strongly nonlinear principal solution. Both force and displacement controlled loadings are considered, the second type of control being necessary for loadings

past the maximum load of the principal solution. The asymptotic results based on the analysis of Section 3 are compared to the exact solution of the problem based on the general theory of Section 2. The presentation is concluded by a discussion in Section 5.

2. Model for the truss structure with out-of-straight deformable members

Although the derivation of the general model for a truss whose members are nonlinear elastic beams is presented in detail by Peek and Triantafyllidis [1992], a self-contained description of the model is included here for reasons of completeness of the presentation.

Without loss of generality, a typical member of the truss is a straight beam of axial stiffness EA, bending stiffness EI and initial length L. The slenderness ratio s is defined as $s^2 \equiv I/AL^2$. In its local coordinate system the beams lies initially along the X axis and deforms in the X, Z plane. The undeformed $\mathbf{R}(X)$ and deformed $\mathbf{r}(X)$ position vectors of the material point initially at distance X from the origin of the beam are given by

$$\mathbf{R}(X) = X\,\mathbf{i}, \qquad \mathbf{r}(X) = [X(1 + e/L) + U(X)]\,\mathbf{i} + [W(X)]\,\mathbf{k} \tag{2.1}$$

where $\mathbf{i}$, $\mathbf{j}$, $\mathbf{k}$ are the unit vectors along the local X, Y, Z axes, and e is the axial elongation of the member. The displacements of the material point X are $[e\,X/L + U(X)]$ and $[W(X)]$ along the X and Z directions respectively. The appropriate strain measures for the beam (*see* Antman [1968]) are the axial strain ε and the bending strain κ, which are given in terms of the undeformed and deformed position vectors in (2.1) by

$$\varepsilon = \|d\mathbf{r}/dX\| - 1, \qquad \kappa = [(d\mathbf{r}/dX) \times \mathbf{j}] \bullet [d^2\,\mathbf{r}/dX^2]/\|d\mathbf{r}/dX\|^2 \tag{2.2}$$

Assuming a linearly elastic response of the beam, its potential energy is given by

$$\phi[e, U, W] = \frac{1}{2}\int_0^L [EA\,\varepsilon^2 + EI\,\kappa^2]\,dX \tag{2.3}$$

where the admissible displacements $U(X)$, $W(X)$ satisfy the simple support boundary conditions

$$U(0) = U(L) = W(0) = W(L) = 0 \tag{2.4}$$

The elongation e is taken as the load parameter of the member. For elongations $0 > e > e_c = -\varepsilon_c L$, where ε_c is the critical axial strain corresponding to the first Euler buckling of the beam under compression, the equilibrium configuration with the minimum potential energy ϕ corresponds to the straight principal solution $(\overset{0}{U}, \overset{0}{W})$

$$\overset{0}{U}(X) = \overset{0}{W}(X) = 0 \tag{2.5}$$

For larger than critical elongations, *i.e.* $e < -\varepsilon_c L$, where the critical strain is the following function of the beam's slenderness s

$$\varepsilon_c = \frac{1}{2}\left[1 - (1 - 4\pi^2 s^2)^{1/2}\right] = \pi^2 s^2 + O(s^4) \tag{2.6}$$

the out-of-straight equilibrium solution (with $U, W \neq 0$) is the one that minimizes ϕ in (2.3). In the following derivations, the LSK (Lyapunov-Schmidt-Koiter) decomposition of the admissible displacements will be employed to find the minimum potential energy at equilibrium. To this end note that at e_c, the buckling mode $(\overset{1}{U}, \overset{1}{W})$ of the axially compressed beam whose potential energy is given by (2.3-4), is

$$\overset{1}{U}(X) = 0, \qquad \overset{1}{W}(X) = \sin(\pi X/L) \tag{2.7}$$

Any admissible displacement (U, W) is decomposed as the sum of a component of amplitude w along the eigenmode $(\overset{1}{U}, \overset{1}{W})$ plus an orthogonal complement $(\overline{U}, \overline{W}) \perp (\overset{1}{U}, \overset{1}{W})$ *i.e.* $\int_0^L (\overset{1}{U}\,\overline{U} + \overset{1}{W}\,\overline{W})\, dX = 0$. For a given elongation e and a fixed amplitude w along the eigenmode, the reduced potential energy at equilibrium $\phi(e, w)$ is

$$\phi(e, w) = \min_{(\overline{U}, \overline{W})} \phi[e, \overline{U}(X), w \sin(\pi X/L) + \overline{W}(X)] \tag{2.8}$$

where in addition to the boundary conditions (2.4), $\overline{W}$ has to satisfy the orthogonality condition $(\overline{U}, \overline{W}) \perp \left(\overset{1}{U}, \overset{1}{W}\right)$ which from (2.7) reduces to

$$\int_0^L \overline{W}(X) \sin(\pi X/L)\, dX = 0 \tag{2.9}$$

For elongations $e < -\varepsilon_c L$ the reduced potential energy $\phi(e, w) \leq \phi(e, 0)$ while the opposite is true for $0 > e > -\varepsilon_c L$. By reducing the infinite d.o.f. potential energy of the beam $\phi[e, U, W]$ in (2.3) to the two degree of freedom equilibrium energy $\phi(e, w)$ in (2.8) (the w d.o.f. for the beam is necessary in view of the bifurcation of the equilibrium path at ε_c) we are capable of describing the truss structure of interest as a finite d.o.f. system. The degrees of freedom of the structure are $u = (v, w)$ where v denotes the set of all the unconstrained nodal displacements of the structure and $w = (w_1, w_2, ..., w_m, ..., w_M)$ denotes the out-of-plane deformation amplitudes of the beams. For a truss with *M* beams, the potential energy $\mathcal{E}$ takes the form †

$$\mathcal{E}(u, \lambda) = \sum_{m=1}^{M} \phi_m(e_m(v), w_m) - \lambda \Delta(v) \tag{2.10}$$

† Note: subscript $(\ )_m$ denotes quantities associated to member m.

It is assumed, without loss of generality, that all external forces are applied proportionally to a load parameter $\lambda \geq 0$ and that its work conjugate displacement quantity $\Delta(v)$ is a linear function of the nodal displacements v. For force control, the value of λ in (2.10) is given, while for displacement control, $\Delta(v)$ is prescribed. In the displacement control case, the $\lambda\Delta(v)$ term in (2.10) is omitted but the constraint $\Delta(v) = \Delta$ is added. The elongation $e_m(v)$ of a beam with initial length L_m and current length l_m and end points corresponding to nodes I, J ‡ of the truss is

$$\text{(2.11)} \qquad \begin{cases} e_m = l_m - L_m, & L_m = \|\Delta \mathbf{x}_m\|, \quad l_m = \|\Delta \mathbf{x}_m + \Delta \mathbf{v}_m\|, \\ & \Delta \mathbf{x}_m = \mathbf{x}_I - \mathbf{x}_J, \quad \Delta \mathbf{v}_m = \mathbf{v}_I - \mathbf{v}_J \end{cases}$$

where $\mathbf{x}_I$ is the reference position vector of node I and $\mathbf{v}_I$ the corresponding displacement, both expressed in the global coordinate system of the truss. To avoid extra notation, from here on λ denotes the control (or load) parameter of the problem in either force or displacement control.

The equilibrium equations of the system are obtained by extremizing $\mathcal{E}$ with respect to u

$$\text{(2.12)} \quad \mathcal{E}_{,u}\,\delta u = \sum_{m=1}^{M} [\phi_{m,e}\, e_{m,v}]\,\delta v - \lambda\Delta(\delta v) + \sum_{m=1}^{M} \phi_{m,w}\,\delta w_m = 0$$

$$\Rightarrow \quad \sum_{m=1}^{M} [N_m\, e_{m,v}]\,\delta v - \lambda\Delta(\delta v) = 0; \qquad \phi_{m,w} = 0, \quad m = 1, \ldots, M.$$

where $N_m \equiv \phi_{m,e}$ is the axial force acting on member m. One can easily show that the principal solution to (2.12) is the one with nodal displacements $v \neq 0$ and straight, *i.e.* only axially deforming, members: $w_m = 0$, $m = 1, \ldots, M$. Indeed by noticing from (2.3), (2.8) that

$$\text{(2.13)} \qquad \begin{cases} \phi(e, 0) = \dfrac{1}{2}(EA/L)\, e^2, & \phi_{,e}(e, 0) = (EA/L)\, e = N(e, 0), \\ & \phi_{,w}(e, 0) = 0 \end{cases}$$

one can see that the principal solution $\overset{0}{u} = (\overset{0}{v}, 0)$ satisfies (2.12) and that $\overset{0}{v}$ is found from

$$\text{(2.14)} \qquad \overset{0}{u} = (\overset{0}{v}, 0); \qquad \sum_{m=1}^{M} (EA/L)_m\, e_m(\overset{0}{v})\, e_{m,v}(\overset{0}{v})\,\delta v - \lambda\Delta(\delta v) = 0$$

The above principal solution $\overset{0}{v}(\lambda)$ obviously satisfies $\overset{0}{v}(0) = 0$ and gives the nodal displacements in a geometrically nonlinear truss (nodal displacements and member rotations can be arbitrarily large) with axially deforming linearly elastic members.

‡ Note: Capital Latin indexes designate node numbers while script Latin indexes designate member numbers.

As the load increases from zero, the principal solution (2.14) loses its stability for some adequately high value of the load parameter λ, termed the critical load. At this point, a number of bifurcated equilibrium solutions emerge from the principal branch. Although all these equilibrium solutions can be found directly by solving (2.12), in the applications of interest the corresponding task can only be performed numerically and presents considerable technical difficulties due to the high number of bifurcated equilibrium paths emerging from the critical load. The asymptotic analysis of these bifurcated equilibrium paths at the neighborhood of the lowest critical load provides an efficient way to study the response of this complicated structure and in particular to determine the shape of the worst imperfection of the structure.

3. Asymptotic analysis for the bifurcated equilibrium solutions of the structure

Of interest here is the behavior of the structure near the lowest load at which the stability of the principal branch is lost. Using (2.14) into (2.12) we find that the wanted critical load λ_c is the lowest value of λ for which the stability operator $\mathcal{E}_{,uu}(\overset{0}{u}(\lambda), \lambda)$ ceases to be positive definite, *i.e.* there exists λ_c and $\overset{i}{u} = (\overset{i}{v}, \overset{i}{w})$ that satisfy

$$(3.1)\quad (\mathcal{E}_{,uu}(\overset{0}{u}(\lambda_c), \lambda_c)\ \overset{i}{u})\,\delta u = \sum_{m=1}^{M} [(EA/L)_m\,(e_{m,v}(\overset{0}{v})\ \overset{i}{v})\,(e_{m,v}(\overset{0}{v})\,\delta v) + (EA/L)_m\,e_m(\overset{0}{v})\,(e_{m,vv}(\overset{0}{v})\ \overset{i}{v})\,\delta v + \phi_{m,ww}(e_m(\overset{0}{v}), 0)\ \overset{i}{w}_m\,\delta w_m] = 0$$

In addition to the first derivatives of ϕ_m with respect to e and w evaluated on the principal branch [*see* (2.13)], the following second derivatives of $\phi(e, w)$ also evaluated on the principal branch have been used in the derivation of (3.1)

$$(3.2)\qquad \phi_{,ee}(e, 0) = EA/L, \qquad \phi_{,ew}(e, 0) = 0$$

An important implication of $(3.2)_2$ is that the equations for the eigenmodes in (3.1) are decoupled, *i.e.* $\mathcal{E}^c_{,vv}\ \overset{i}{v}\ \delta v = 0$, $\mathcal{E}^c_{,ww}\ \overset{i}{w}\ \delta w = 0$.† The first equation characterizes the stability of the equilibrium solution when no out-of-straight deformation is allowed in the members, while the second one determines the stability of the same equilibrium solution when all nodes are fixed. If $\mathcal{E}^c_{,vv}$ is singular, then $\overset{i}{v} \neq 0$ and global buckling modes or limit load points can develop in the truss while all its members remain straight. In this work, interest is focused only on structures where the local Euler buckling of several

† Note: From here and subsequently a superscript $(\ )^c$ or subscript $(\ )_c$ denotes a quantity evaluated at the critical point on the principal branch (λ_c, u_c) (*i.e.* the point that corresponds to the first Euler buckling of the bars with the highest axial load), while a superscript $(\ )^0$ or subscript $(\ )_0$ denotes a quantity evaluated at any point on the principal branch $\overset{0}{u}(\lambda)$.

members precedes the first global buckling. Consequently it is assumed that

$$
\begin{cases}
(\mathcal{E}^c_{,vv}\,\delta v)\,\delta v > 0 \quad \Rightarrow \quad \displaystyle\sum_{m=1}^{M} [(EA/L)_m\,(e_{m,v}(\overset{0}{v})\,\delta v)^2 \\
\qquad\qquad + N_m(\overset{0}{e}_m, 0)(e_{m,vv}(\overset{0}{v})\,\delta v)\,\delta v] > 0, \\
\qquad 0 \le \lambda \le \lambda_c, \qquad \delta v \neq 0 \\
(\mathcal{E}^c_{,ww}\,\overset{i}{w})\,\delta w = 0 \quad \Rightarrow \quad \phi_{m,ww}(\overset{0}{e}_m(\lambda_c), 0) = 0, \\
\qquad \overset{0}{e}_m(\lambda_c) = -\varepsilon_c L_m, \qquad m \in \mathcal{G}
\end{cases}
\tag{3.3}
$$

At load λ_c, the set of members that reach simultaneously their lowest Euler buckling load $N^c_m = (EA/L)_m\,\varepsilon_c$ is denoted by $\mathcal{G}$. The corresponding elongation for each member is $\overset{0}{e}_m(\lambda_c) = -\varepsilon_c L_m$, $m \in \mathcal{G}$ where ε_c, the lowest critical strain in compression for the axially loaded simply supported beam, is given by (2.6). For symmetric structures with a large number of identical members and under symmetric loading, there exist sets of identical members that have the same principal strain $\overset{0}{e}_m(\lambda)/L_m$. As the loading increases, one of the these groups of identical members under same strain will first reach the corresponding lowest Euler buckling load. In view of the assumption in $(3.3)_1$, there exist at λ_c a set of simultaneous eigenmodes $\overset{i}{u}$, $i \in \mathcal{G}$, of the form

$$
\begin{cases}
\qquad\qquad \overset{i}{u} = (\overset{i}{v}, \overset{i}{w}); \\
\overset{i}{v} = 0, \qquad \overset{i}{w} = (\overset{i}{w}_1, \overset{i}{w}_2 \ldots \overset{i}{w}_m \ldots \overset{i}{w}_M) \quad \begin{cases} \overset{i}{w}_m = 0 & \text{for } m \neq i \\ \overset{i}{w}_m \neq 0 & \text{for } m = i \in \mathcal{G} \end{cases}
\end{cases}
\tag{3.4}
$$

The fact that the $\overset{i}{u}$ in (3.4) correspond to a multiple bifurcation of the system at λ_c and not a limit point can be easily confirmed by assuring the necessary, according to the general theory (*see* Triantafyllidis and Peek [1992]), condition for a multiple bifurcation at criticality $\mathcal{E}^c_{,u\lambda}\,\overset{i}{u} = 0$. Indeed form (2.12), (3.4)

$$
\mathcal{E}^c_{,u\lambda}\,\overset{i}{u} = -\Delta(\overset{i}{v}) = 0 \tag{3.5}
$$

One can identify the null space $\mathcal{N}$ and its complement $\mathcal{N}^\perp$ at the critical point (λ_c, u_c). In view of (3.4)

$$
\mathcal{N} \equiv \{u = (v, w) | w_i \neq 0\ i \in \mathcal{G},\ w_i = 0\ i \notin \mathcal{G},\ v = 0\}
$$
$$
\mathcal{N}^\perp \equiv \{u = (v, w) | w_i = 0\ i \in \mathcal{G},\ w_i \neq 0\ i \notin \mathcal{G},\ v \neq 0\}
$$

Obviously each one of the eigenmodes is a local one since it involves the out-of-straight buckling of one member while leaving the rest of the structure intact (the eigenmode

evaluated at all the other degrees of freedom vanishes). The amplitude $\overset{i}{w}_i$ of eigenmode $\overset{i}{w}$ is chosen so that $\mathcal{E}_{ij\lambda} = -\phi_r \delta_{ij}$, where $\phi_r > 0$ is a constant specifiable below. From (2.8), (3.1), (3.4)

$$(3.6)\quad \begin{cases} \mathcal{E}_{ij\lambda} \equiv ((d\mathcal{E}_{,uu}/d\lambda)_c \overset{i}{u})\overset{j}{u} = \dfrac{\pi^2}{2L_i}\dfrac{1-2\varepsilon_c}{(1-\varepsilon_c)^2}(d\overset{0}{N}_I/d\lambda)_c(\overset{i}{w}_i)^2\delta_{ij} = -\phi_r\delta_{ij} \\ \phi_r = \dfrac{\pi^2}{2\lambda_c}\dfrac{1-2\varepsilon_c}{(1-\varepsilon_c)^2}N_r L_r, \qquad \overset{i}{w}_i = \{L_i L_r N_r/[-\lambda_c(d\overset{0}{N}_i/d\lambda)_c]\}^{1/2} \end{cases}$$

where L_r, N_r are a conveniently chosen reference length and a reference force respectively. A specific choice for L_r and N_r will be adopted in the results section. Moreover, in the derivation of (3.6) use was made of the result, obtained by direct calculations from (2.8) (*see* Triantafyllidis and Peek [1992])

$$(3.7)\qquad \phi_{,eww}(e_c, 0) = \frac{\pi^2 EA}{2L^2}\frac{1-2\varepsilon_c}{(1-\varepsilon_c)^2}$$

As expected from the general theory (*see* Triantafyllidis and Peek [1992]) $-\mathcal{E}_{ij\lambda}$ in (3.6) should be a positive definite matrix. Consequently we must assure that the compressive axial forces $\overset{0}{N}_i(\lambda)$ increase in absolute value, at least for the bars that reach their lowest buckling load at λ_c. Hence it is assumed that $(d\overset{0}{N}_i/d\lambda)_c < 0$, $i \in \mathcal{G}$.

In view of the fact that on the principal branch (2.8) gives

$$(3.8)\qquad \phi_{,www}(e, 0) = 0$$

one can thus conclude from (3.1), (3.4), (3.8) that the coefficients $\mathcal{E}_{ijk}$ (*see* the general theory in Triantafyllidis and Peek [1992] for further details) vanish, *i.e.*

$$(3.9)\qquad \mathcal{E}_{ijk} \equiv ((\mathcal{E}^c_{,uuu}\overset{i}{u})\overset{j}{u})\overset{k}{u} = \sum_{i\in\mathcal{G}} \phi^c_{i,www}(\overset{i}{w}_i)^3 = 0$$

Consequently the multiple bifurcation at λ_c is a symmetric one. In order to find out the initial directions $\{\alpha^1_i\}$, $i \in \mathcal{G}$, of the bifurcated equilibrium branches emerging from λ_c, one has to calculate according to the general theory (*see* Triantafyllidis and Peek [1992]), the second order displacements $\overset{ij}{v}$ defined by

$$(3.10)\qquad (\mathcal{E}^c_{,uu}\overset{ij}{v} + (\mathcal{E}^c_{,uuu}\overset{i}{u})\overset{i}{u})\delta v = (\mathcal{E}^c_{,vv}\overset{ij}{v})\delta v + ((\mathcal{E}^c_{,vww}\overset{i}{w})\overset{j}{w})\delta v = 0$$

where $\mathcal{E}^c_{,vv}$, the tangent stiffness matrix of the constrained against out-of-straight deformations truss at λ_c, is given by $(3.3)_1$. With the help of (3.4), (3.7), one can deduce that $\overset{ij}{v} = 0$ for $i \neq j$ while for $i = j$ (3.10) simplifies to

$$(3.11)\qquad (\mathcal{E}^c_{,vv}\overset{ii}{v})\delta v + \phi^c_{i,eww}(\overset{i}{w}_i)^2(e^c_{i,v}\delta v) = 0$$

where $\mathcal{E}^c_{,vv}$, $\overset{i}{w}_i$ and $\phi^c_{i,eww}$ are given by $(3.3)_1$, $(3.6)_3$ and (3.7) respectively. Due to the assumed positive definiteness of $\mathcal{E}^c_{,vv}$ (no global buckling occurs until after λ_c) a unique solution $\overset{ii}{v}$ to (3.11) is assured. With the help of (3.11) we can calculate the final ingredient required in the determination of the initial directions of the bifurcated equilibrium branches emerging from λ_c, namely the coefficients $\mathcal{E}_{ijkl}$. From (2.12-14) and (3.1-4) on finds

$$
\text{(3.12)} \qquad \begin{cases} \mathcal{E}_{ijkl} \equiv (((\mathcal{E}^c_{,uuuu}\ \overset{j}{u})\ \overset{k}{u})\ \overset{l}{u} + (\mathcal{E}^c_{,uuu}\ \overset{jk}{v})\ \overset{l}{u} + (\mathcal{E}^c_{,uuu}\ \overset{jl}{v})\ \overset{k}{u} \\ \qquad\qquad + (\mathcal{E}^c_{,uuu}\ \overset{kl}{v})\ \overset{j}{u})\ \overset{i}{u} = \phi_r\,[a_{ik}\,\delta_{ij}\,\delta_{kl} + a_{il}\,\delta_{ik}\,\delta_{jl} + a_{ij}\,\delta_{il}\,\delta_{jk}] \\ a_{ij} \equiv \left[\dfrac{1}{3}\,\phi^c_{i,wwww}\,(\overset{i}{w}_i)^4\,\delta_{ij} + \phi^c_{i,eww}\,(\overset{i}{w}_i)^2\,e_{i,v}\,(\overset{jj}{v})\right]/\phi_r \end{cases}
$$

where $\phi^c_{i,eww}$ is given in (3.7) and $\phi^c_{i,wwww}$ is found from (2.8) to be

$$
\text{(3.13)} \qquad \phi_{,wwww}\,(e_c,\,0) = \frac{\pi^4\,EA}{8\,L^3}\,\frac{6 - 21\,\varepsilon_c + 12\,\varepsilon_c^2}{(1-\varepsilon_c)^4}
$$

Notice that the coefficients a_{ij} defined in $(3.12)_2$ are symmetric, a property easily verified by taking $\delta v = \overset{jj}{v}$ in (3.11). According to the general theory in Triantafyllidis and Peek [1992], the asymptotic form of the bifurcated equilibrium paths of the structure at λ_c are given in term of the amplitude parameter ξ by

$$
\text{(3.14)} \qquad \begin{cases} \lambda(\xi) = \lambda_c + \dfrac{1}{2}\,\lambda_2\,\xi^2 + O(\xi^3), \qquad u = (\overset{0}{v}\ (\lambda(\xi)) + v(\xi),\, w(\xi)). \\ v(\xi) = \dfrac{1}{2}\,\xi^2 \displaystyle\sum_{i\in\mathcal{G}} (\alpha^1_i)^2\ \overset{ii}{v} + O(\xi^3), \quad w(\xi) = (w_1(\xi),\, w_2(\xi) \ldots w_i(\xi) \ldots w_M(\xi)) \\ w_i(\xi) = \xi\alpha^1_i + O(\xi^3) \quad \text{for } i \in \mathcal{G}, \qquad w_i(\xi) = 0 \quad \text{for } i \notin \mathcal{G}. \end{cases}
$$

The components $\{\alpha^1_i\}$ of the tangent to the bifurcated paths are given, according to the general theory in Triantafyllidis and Peek [1992], by the solution to the system

(3.15)

$$
\begin{cases} \displaystyle\sum_{j\in\mathcal{G}} 3\,\lambda_2\,\alpha^1_j\,\mathcal{E}_{ij\lambda} + \sum_{j\in\mathcal{G}}\sum_{k\in\mathcal{G}}\sum_{l\in\mathcal{G}} \alpha^1_j\,\alpha^1_k\,\alpha^1_l\,\mathcal{E}_{ijkl} = 3\,\phi_r\,\alpha^1_i\,[-\lambda_2 + \sum_{j\in\mathcal{G}} a_{ij}\,(\alpha^1_j)^2] = 0, \\ \displaystyle\sum_{j\in\mathcal{G}} (\alpha^1_j)^2 = 1 \end{cases}
$$

The solution to the above system can be obtained as follows: For each solution of (3.15), we partition the set $\mathcal{G}$ of members that have reached their Euler buckling load at λ_c in two mutually exclusive and collectively exhaustive sets $\mathcal{G}_0$, $\mathcal{G}_1$. The set $\mathcal{G}_0$ contains all

the bars that remain straight in the bifurcated equilibrium path in question, *i.e.* $\alpha_i^1 = 0$ if $i \in \mathcal{G}_0$, while the set $\mathcal{G}_1$ contains all the bars that buckle in the bifurcated equilibrium path in question, *i.e.* $\alpha_i^1 \neq 0$ if $i \in \mathcal{G}_1$. Consequently, each solution of (3.15), can equivalently be put in the form

$$\text{(3.16)} \qquad \begin{cases} \alpha_i^1 = 0, \qquad i \in \mathcal{G}_0; \qquad \displaystyle\sum_{j \in \mathcal{G}_1} a_{ij}\, y_j = 1, \qquad \alpha_i^1 = \pm\, [y_i / \sum_{j \in \mathcal{G}_1} y_j]^{1/2}, \\ \qquad\qquad\qquad\qquad \lambda_2 = [\displaystyle\sum_{j \in \mathcal{G}_1} y_j]^{-1}, \qquad i \in \mathcal{G}_1 \end{cases}$$

where y_i, $i \in \mathcal{G}_1$, is a set of same sign numbers. Each such solution of (3.16) gives the initial tangent $\{\alpha_i^1\}$ of the corresponding bifurcated equilibrium path. The initial stability of each one of these equilibrium paths is, according to the general theory in Triantafyllidis and Peek [1992], determined by the positive definiteness of the stability matrix B_{ij}

$$\text{(3.17)} \qquad B_{ij} \equiv \lambda_2\, \mathcal{E}_{ij\,\lambda} + \sum_{k \in \mathcal{G}} \sum_{l \in \mathcal{G}} \mathcal{E}_{ijkl}\, \alpha_k^1\, \alpha_l^1$$

$$= \begin{cases} [-\lambda_2 + \displaystyle\sum_{k \in \mathcal{G}_1} a_{ik}\, (\alpha_k^1)^2]\, \phi_r\, \delta_{ij} & \text{if} \quad i \text{ or } j \in \mathcal{G}_0 \\ [2\, a_{ij}\, \alpha_i^1\, \alpha_j^1]\, \phi_r & \text{if} \quad i \text{ and } j \in \mathcal{G}_1 \end{cases}$$

A bifurcated equilibrium branch is termed "*locally stable*" if its non-buckling members are stable, which from (3.17) implies $B_{ii} \geq 0$ for $i \in \mathcal{G}_0$ and since $\phi_r > 0$

$$\text{(3.18)} \qquad -\lambda_2 + \sum_{j \in \mathcal{G}_1} a_{ij}\, (\alpha_j^1)^2 \geq 0, \qquad i \in \mathcal{G}_0$$

If the above condition is satisfied for all non-buckling members of a bifurcated solution, the stability of each such member implies that the magnitude of the compressive axial load on that bifurcated branch is reduced from its critical value at bifurcation, *i.e.* it is less than the first Euler load. Notice however that local stability of a bifurcated equilibrium solution does not imply its overall stability since the matrix of coefficients $[a_{ij}\, \alpha_i^1\, \alpha_j^1]$ for $i, j \in \mathcal{G}_1$ is not in general a positive definite matrix.

Of interest is the bifurcated equilibrium solution for which the corresponding λ_2 [*see* $(3.15)_1$ or $(3.16)_4$] assumes the minimum possible value $(\lambda_2)_{\min}$. According to the general theory (*see* Triantafyllidis and Peek [1992]) an imperfection whose projection on the null space is on the direction of the above mentioned lowest λ_2 branch, will produce the maximum load drop $\Delta\lambda_s \equiv \lambda_m - \lambda_c$, defined as the difference between the critical load λ_c and the first load maximum of the imperfect equilibrium solution λ_m, assuming an adequately small imperfection.

A preferable alternative to solve (3.16) for the minimum $(\lambda_2)_{\min}$ is the equivalent constrained quadratic minimization formulation

$$\text{(3.19)} \qquad (\lambda_2)_{\min} = \min\, [\sum_{i \in \mathcal{G}} \sum_{j \in \mathcal{G}} a_{ij}\, x_i\, x_j]; \qquad \sum_{i \in \mathcal{G}} x_i = 1, \qquad x_i \geq 0, \quad i \in \mathcal{G}$$

where $x_i \equiv (\alpha_i^1)^2$. Despite the simple appearance of the minimization problem, it may have many local minima, since the matrix of coefficients is not in general definite (positive or negative). Indeed any solution to (3.16) is a potential local minimum. Fortunately in applications, as we will see in the examples of the following Section, the actual number of local minima is much smaller.

An interesting property of the local minima of (3.19) is that the corresponding solutions are locally stable in the sense of (3.18). The proof goes as follows: Suppose that the inequality constraints $x_i \geq 0$ are replaced by the more restrictive ones $x_i \geq b_i$ where $b_i \geq 0$ and that these constraints are active for all $i \in \mathcal{G}_0$. If b_i is increased for some $i \in \mathcal{G}_0$ then the inequality constraint becomes more restrictive and thus the corresponding minimal value λ_2 should increase. Thus a necessary condition for optimality is $\partial\lambda_2/\partial b_i \geq 0$. On the other hand, one can define the Lagrangian $\mathcal{L}$

$$\mathcal{L} = \sum_{i\in\mathcal{G}} \sum_{i\in\mathcal{G}} a_{ij}\, x_i\, \alpha_j + \mu\,(\sum_{i\in\mathcal{G}} x_i - 1) + \sum_{i\in\mathcal{G}_0} \mu_i\,(x_i - b_i) \tag{3.20}$$

which at the local minimum λ_2 is stationary with respect to x_i, μ_i and μ. From stationarity of $\mathcal{L}$ with respect to $x_i\,(i \in \mathcal{G}_1)$ one recovers (3.15) which leads to

$$2 \sum_{j\in\mathcal{G}} a_{ij}\, x_j + \mu = 0, \qquad \mu = -2\,\lambda_2, \qquad i \in \mathcal{G}_1 \tag{3.21}$$

Using $(3.21)_2$, stationarity of $\mathcal{L}$ with respect to $x_i\,(i \in \mathcal{G}_0)$ gives

$$2\,(\sum_{i\in\mathcal{G}} a_{ij}\, x_j - \lambda_2) = -\mu_i = \frac{\partial\lambda_2}{\partial b_i} \geq 0, \quad i \in \mathcal{G}_0 \tag{3.22}$$

For the case $b_i = 0$ the $\sum_{j\in\mathcal{G}}$ reduces to $\sum_{j\in\mathcal{G}_1}$ and (3.22) coincides with the local stability condition in (3.18).

4. Application to structures with nonlinear principal solution

The theory presented in the previous section will be used to investigae the post-buckling behavior of truss structures where a number of bars reach their lowest buckling load simultaneously. In the structures considered, the principal solution of the truss, in which all members remain straight, is a nonlinear function of the loading parameter. Moreover, the simultaneous buckling of a number of bars in the truss occurs in the stable regime of the principal solution, *i.e.* the load parameter at which local buckling occurs in several members of the truss is lower than the load parameter corresponding to the first bifurcation of the nonlinear principal solution. This is typically the case in structural applications where, due to the symmetry of the structure's geometry and loading, the set of elements under the highest compressive forces reach their first Euler buckling at load parameters well before the lowest critical one of the principal solution.

Depending on the bending stiffness *EI* of the members of the truss, and under the tacit assumption that all members' axial stiffness *EA* is fixed, the members with the highest axial force can buckle at any value of the loading parameter of the system. Of interest is the dependence of $(\lambda_2)_{\min}$, which corresponds to the most imperfection sensitive (according to the general asymptotic analysis presented in Triantafyllidis and Peek [1992]) bifurcated equilibrium branch of the structure, on the loading parameter. In addition, the bifurcated equilibrium branches of some of these structures are calculated based on the exact analysis of Section 2 and compared with the asymptotic results of Section 3 in order to investigate the range of validity of these asymptotic results.

The structures studied are regular hexagonal dome-like trusses whose projection onto the $x-y$ plane forms a regular grid of equilateral triangles as seen in Figures 1 and 2. This grid of equilateral triangles is inscribed inside a circle of radius $N_S \times R$, where R is the sidelength of the equilateral triangles. Thus $N_S = 1$ for the dome depicted in Figure 1 (the "*one storey dome*"), and $N_S = 2$ for the dome depicted in Figure 2 (the "*two storey dome*"). Each dome has a height of $N_S \times H$ and the z-coordinate of the nodes labeled A_i for $N_S = 2$ is $2H(1-8^{-1/2})$. The structures are loaded by forces of magnitude λ along the $-z$ directions as shown. All bars are taken to have the same axial stiffness *EA* and bending stiffness *EI*. The trusses are supported by rollers at the $z = 0$ plane (*i.e.* only the vertical displacement of each base node is constrained to be zero). In addition, the rigid body motion is precluded by constraining the x and y displacements of node A_4 for $N_S = 1$ or B_4 for $N_S = 2$ and the y displacement of node A_1 for $N_S = 1$ or B_1 for $N_S = 2$.

The work conjugate quantity $\Delta(v)$ to the load parameter λ under force control, is the sum of all the z displacements of the external local carrying nodes. A penalty method is employed to solve for the principal solution $\overset{0}{v}(\Delta)$ when $\Delta(v) = \Delta$ is prescribed as the load parameter, according to which the term $\lambda\Delta(v)$ is replaced by $\rho(\Delta(v)-\Delta)^2/2$ where ρ is a large positive number. In the numerical calculations reported here $\rho/EA = 10^7$ although values ranging from 10^6 to 10^9 gave no appreciable difference in the results (less than 0.1%). In all the subsequent calculations, the reference length introduced for mode normalization purposes in (3.6) is taken to be $L_r = R$, while N_r is always chosen to ensure the maximum amplitude $(\overset{i}{w}_i)_{\max} = L_r$.

As previously stated, all the bars of the structure have the same axial *EA* and bending *EI* stiffnesses. By varying the slenderness s of the members, (recall $s \equiv I/AL^2$), we can obtain a local type bifurcation mode at any level of prestrain. Of interest is the dependence of the imperfection sensitivity of such a space structure on the slenderness ratio of the beams, or equivalently, on the level of prestrain, when the truss geometry is kept fixed. The imperfection sensitivity can be determined from the analysis of the perfect structure, by finding the bifurcated equilibrium path with the most rapid load drop, and is measured by the initial curvature of the corresponding bifurcated equilibrium path $|(\lambda_2/\lambda_c)_{\min}|$ (for force control) or $|(\Delta_2/R)_{\min}|$ (for displacement control).

As previously mentioned, all the space trusses investigated have numbers with identical properties. Hence the bars that buckle at the critical load are the ones

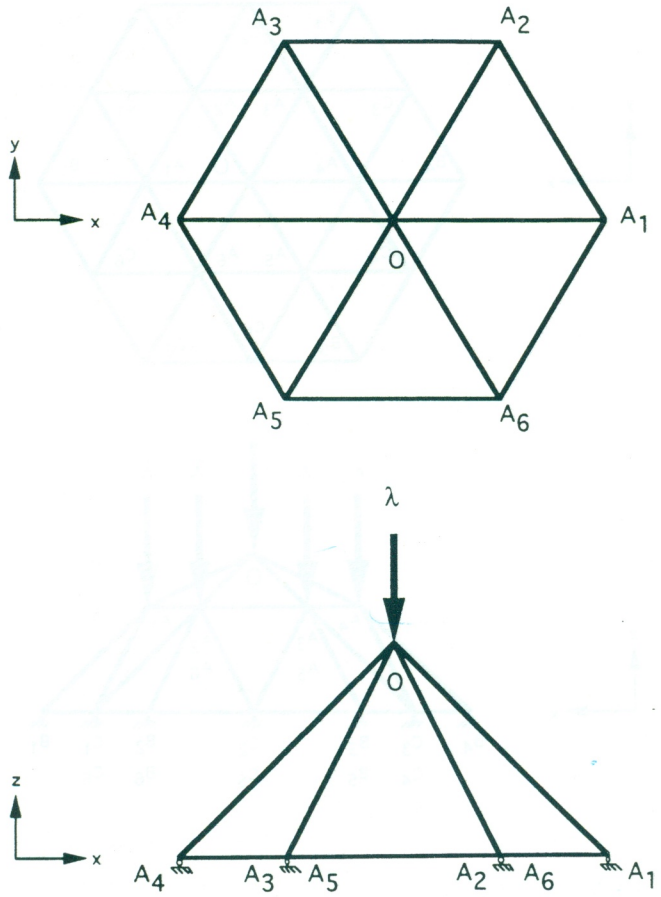

Fig. 1. – Geometry and loading of the twelve member "*one storey dome*" truss $N_S = 1$. The projections of all bars in the $x - y$ plane have length R and the height of the dome (z coordinate of the center node 0) is H.

with the highest compressive forces. For the one storey done in Figure 1, and for all the values of the load parameter considered, the set of simultaneously buckling bars is $\mathcal{G} = \{OA_1, OA_2, OA_3, OA_4, OA_5, OA_6\}$. The same bars are the simultaneously buckling bars for the two storey dome in Figure 2 when only one force is applied at the apex ($N_L = 1$). However, when seven equal forces are applied on the dome ($N_L = 7$), the simultaneously buckling bars are different and in this case $\mathcal{G} = \{A_1 B_1, A_2 B_2, A_3 B_3, A_4 B_4, A_5 B_5, A_6 B_6\}$. Since all the simultaneously buckling bars have always identical properties and principal loadings, the choice of the mode normalization reference force N_r ensures that all the eigenmodes have the same amplitude, $\overset{i}{w}_i = L_r$, $(i \in \mathcal{G})$.

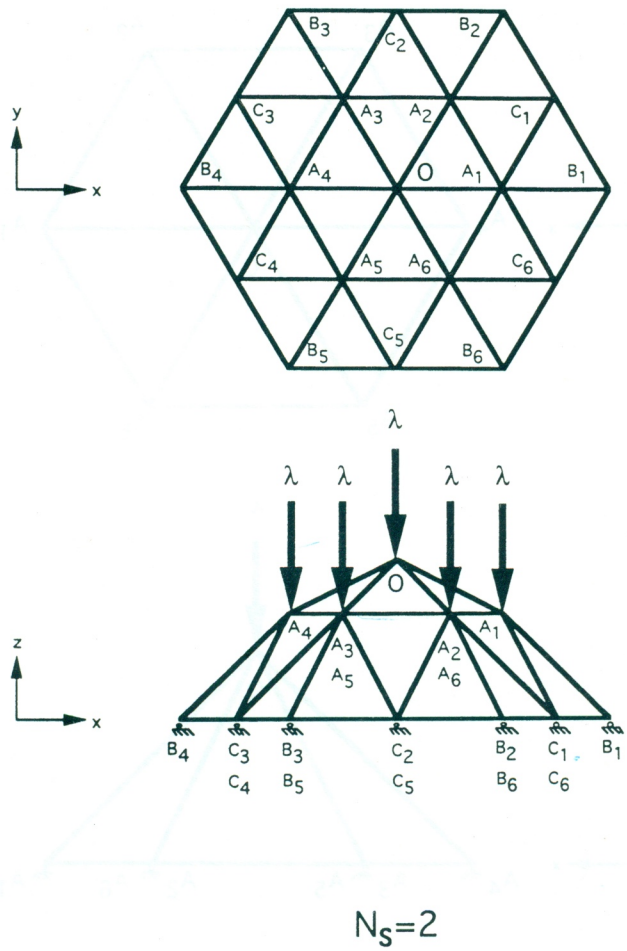

Fig. 2. – Geometry and loading of the forty two member "*two storey dome*" truss $N_S = 2$. The projections of all bars in the $x - y$ plane have length R and the height of the dome (z coordinate of the center node 0) is $2\,H$. The height (z coordinate) of nodes A_i is $2\,H\left(1 - 8^{-1/2}\right)$.

The dependence of the minimum $(\Delta_2/R)_{\min}$ on Δ/R for the displacement (Δ/R) controlled loading of the one storey $(N_S = 1)$ shallow dome of height $H/R = 0.1$ is presented in Figure 3a. The dependence of the minimum $(\lambda_2/\lambda_c)_{\min}$ on Δ/R for the force (λ/EA) controlled loading of the same dome is presented in Figure 3b. There is no global buckling mode of the truss for apex displacements Δ in the range $0 \leq \Delta \leq H$ (note that for apex loaded structures, $N_L = 1$, $\Delta = \Delta\,(v)$ is the apex displacement). The principal solution of this structure exhibits according to Figure 3c a load maximum just prior to $\Delta/R = 0.05$, which explains why the load control results in Figure 3b are calculated for $\Delta/R \leq 0.04$. For the displacement control case, $\Delta = 0.1\,R = H$ is a singular point of the principal solution, in the sense that $dN_i/d\Delta = 0$, $(i \in \mathcal{G})$. Hence for the adopted mode normalization condition at $\Delta/R = 0.1$ we obtain $\phi_r = 0$ which in turn implies from (3.12) that $a_{ij} \to \infty$ and from (3.19) that $\Delta_2 \to \infty$, thus explaining the vertical asymptote in Figure 3a. For force controlled loading, $(\lambda_2)_{\min} < 0$

and its absolute value increases with increasing loading. Since the maximum load drop of the imperfect structure is proportional to $(\lambda_2)_{\min}$ (recall from the general theory in Triantafyllidis and Peek [1992] $(\Delta\lambda_s)_{\max}/\lambda_c = (3/2)[(\lambda_2/\lambda_c)_{\min}\,\varepsilon^2]^{1/3} + O(\varepsilon)$) the imperfection sensitivity of the load controlled shallow dome increases monotonically with increasing prestrain. The situation is different for the displacement controlled shallow dome since $(\Delta_2)_{\min} > 0$, which implies that the structure is no longer imperfection

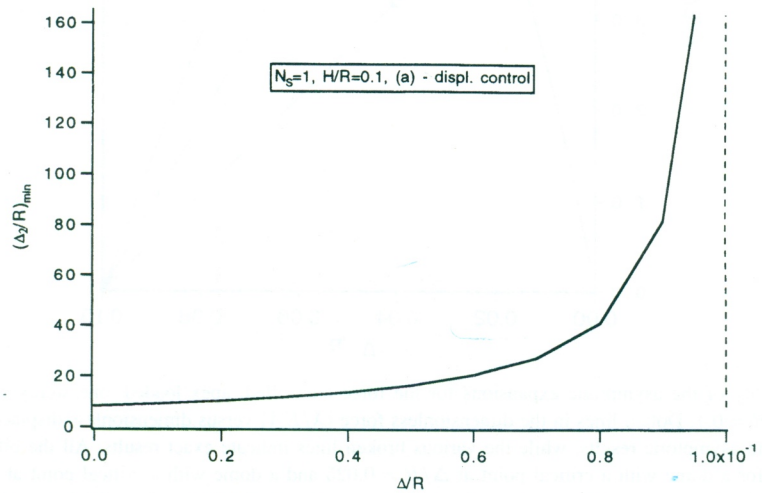

Fig. 3 a. – Imperfection sensitivity of the apex loaded one storey shallow dome, $N_S = 1$, $H/R = 0.1$, based on the equilibrium path with the steepest load drop of the perfect structure. Graph corresponds to the displacement controlled loading and gives $(\Delta_2/R)_{\min}$ as a function of the displacement (Δ/R).

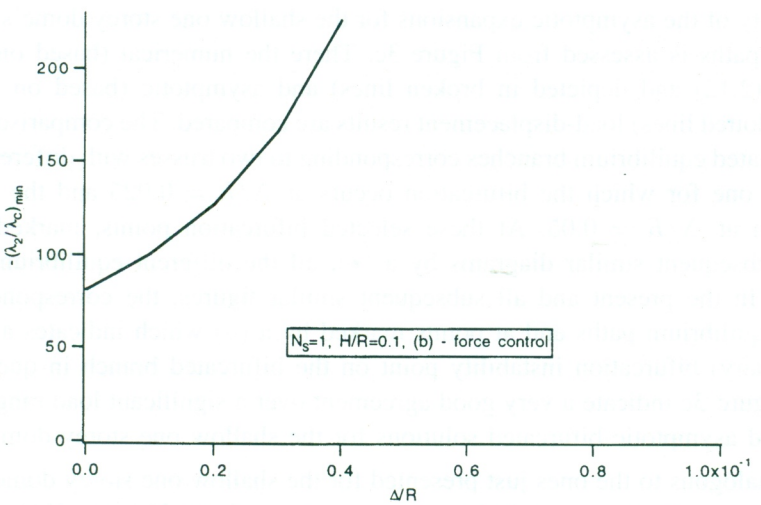

Fig. 3 b. – Imperfection sensitivity of the apex loaded one storey shallow dome, $N_S = 1$, $H/R = 0.1$, based on the equilibrium path with the steepest load drop of the perfect structure. Graph corresponds to the force controlled loading and gives $-(\lambda_2/\lambda_c)_{\min}$ as a function of the displacement (Δ/R).

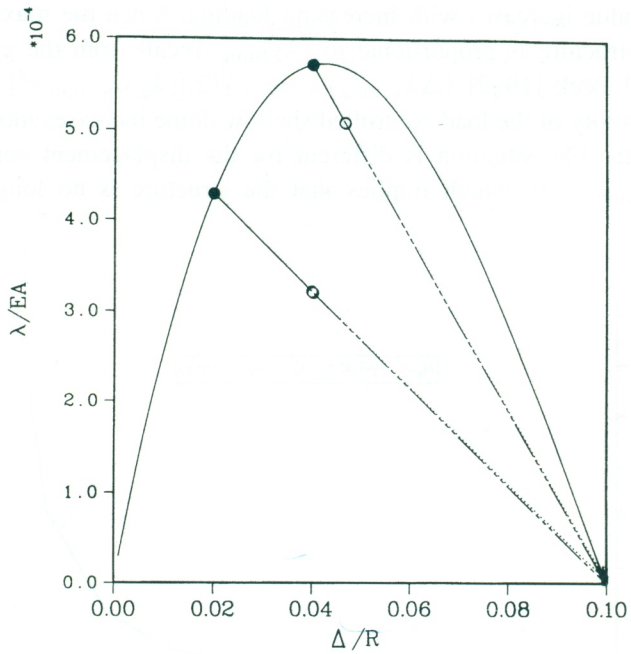

Fig. 3 c. – Validity of the asymptotic expansions for the force controlled, apex loaded, one storey shallow dome, $N_S = 1$, $H/R = 0.1$. Dotted lines in the dimensionless force (λ/EA) versus dimensionless displacement (Δ/R) graphs indicate asymptotic results, while the various broken lines indicate exact results. All the bifurcated paths were plotted for a dome with a critical point at $\Delta/R = 0.025$ and a dome with a critical point at $\Delta/R = 0.05$. The $(\circ)$ denotes the first instability found in the numerically calculated bifurcated equilibrium paths.

sensitive, at least in the asymptotic sense, since all the bifurcated equilibrium branches are supercritical, *i.e.* they occur at $\Delta > \Delta_c$.

The validity of the asymptotic expansions for the shallow one storey dome's bifurcated equilibrium paths is assessed from Figure 3c. There the numerical (based on the exact solution of (2.12) and depicted in broken lines) and asymptotic (based on (3.14) and depicted in dotted lines) load-displacement results are compared. The comparison involves all the bifurcated equilibrium branches corresponding to two trusses with different member slenderness: one for which the bifurcation occurs at $\Delta/R = 0.025$ and the other with a bifurcation at $\Delta/R = 0.05$. At these selected bifurcation points, marked here and in all the subsequent similar diagrams by a $(\bullet)$, all the different equilibrium branches are plotted. In the present and all subsequent similar figures, the corresponding exact bifurcated equilibrium paths end at points marked by a $(\circ)$ which indicates a limit load or a (secondary) bifurcation instability point on the bifurcated branch in question. The results in Figure 3c indicate a very good agreement over a significant load range between the exact and asymptotic bifurcated solutions for the shallow one storey dome.

Results analogous to the ones just presented for the shallow one storey dome are given next in Figures 4a, 4b and Figure 4c for a steep one storey dome $N_S = 1$, $H/R = 1.5$. The dependence of $(\Delta_2/R)_{\min}$ on Δ/R for the displacement controlled loading is depicted in Figure 4a while the corresponding results for $(\lambda_2/\lambda_c)_{\min}$ for the force controlled loading

of the same structure are presented in Figure 4b. Similarly to the shallow dome case, there is a load maximum at $\Delta/R = 0.69$ while the $dN_i/d\Delta = 0$, $(i \in \mathcal{G})$ singularity appears as expected in the flattened-out configuration with $\Delta = 1.5\,R = H$. In contrast to the shallow one storey dome case, notice in Figure 4b that the absolute value of $(\lambda_2)_{\min}$ is no longer monotonically increasing with the increasing compression of its members. Notice also that the dome whose bars buckle at $\Delta/R = 0.69$ is considerably less imperfection sensitive than the one whose bars buckle at $\Delta/R = 0.3$. Another significant difference with the shallow one storey dome is that for approximately $\Delta/R > 0.2$,

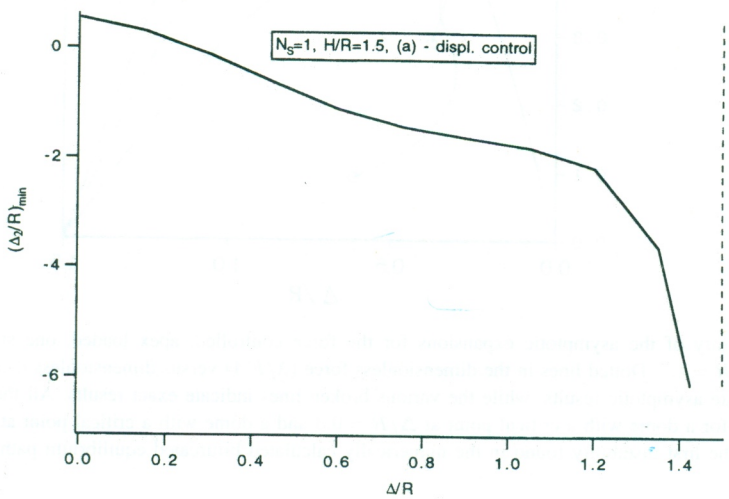

Fig. 4 a. – Imperfection sensitivity of the apex loaded one storey steep dome, $N_S = 1$, $H/R = 1.5$, based on the equilibrium path with the steepest load drop of the perfect structure. Graph corresponds to the displacement controlled loading and gives $(\Delta_2/R)_{\min}$ as a function of the displacement (Δ/R).

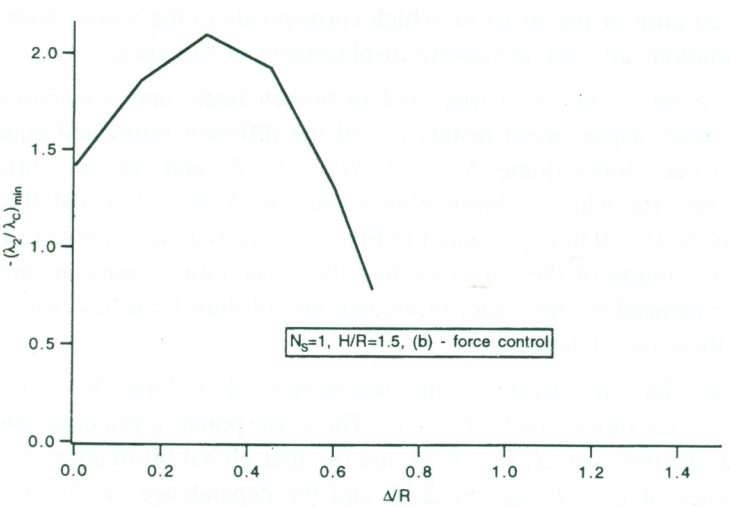

Fig. 4 b. – Imperfection sensitivity of the apex loaded one storey steep dome, $N_S = 1$, $H/R = 1.5$, based on the equilibrium path with the steepest load drop of the perfect structure. Graph corresponds to the force controlled loading and gives $-(\lambda_2/\lambda_c)_{\min}$ as a function of the displacement (Δ/R).

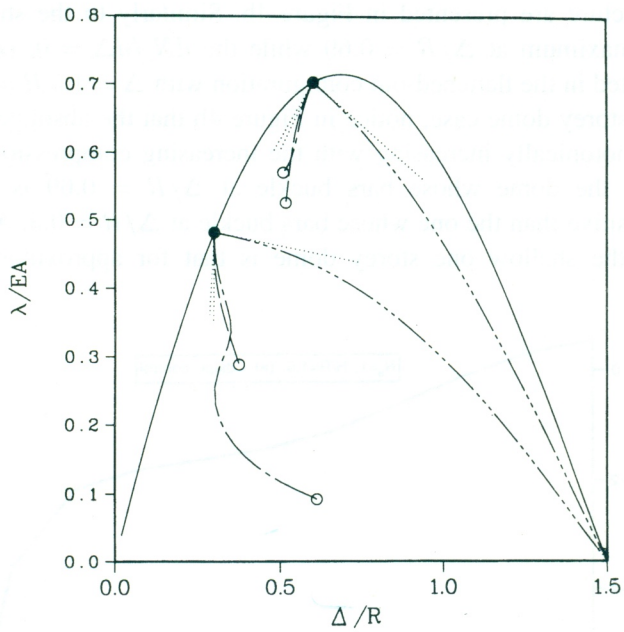

Fig. 4 c. – Validity of the asymptotic expansions for the force controlled, apex loaded, one storey steep dome, $N_S = 1$, $H/R = 1.5$. Dotted lines in the dimensionless force (λ/EA) versus dimensionless displacement (Δ/R) graphs indicate asymptotic results, while the various broken lines indicate exact results. All the bifurcated paths were plotted for a dome with a critical point at $\Delta/R = 0.3$ and a dome with a critical point at $\Delta/R = 0.6$. The $(\circ)$ denotes the first instability found in the numerically calculated bifurcated equilibrium paths.

$(\Delta_2)_{\min} < 0$ which implies that the steep dome structure under displacement control is also imperfection sensitive. Thus for $\Delta/R > 0.2$ the imperfection sensitivity, *i.e.* the maximum load drop of the structure which corresponds to the worst shape imperfection, increases monotonically for increasing displacement at the apex.

The comparison of the exact (depicted in broken lines) and asymptotic (depicted in dotted lines) load-displacement results for all the different bifurcated equilibrium paths for the steep one storey dome $N_S = 1$, $H = 1.5\,R$, and for two different member slenderness: one for which a bifurcation occurs at $\Delta/R = 0.3$ and the other with a bifurcation at $\Delta/R = 0.6$, is presented in Figure 4c. Notice, in contrast to Figure 3c, that the regions of validity of the corresponding the asymptotic expansions are considerably smaller, as evidenced by the exact bifurcated equilibrium branches that rapidly deviate away from their initial tangents.

The next structure investigated is the two story shallow dome $N_S = 2$, $H = 0.2\,R$ in Figure 2 under one (apex) load $(N_L = 1)$. The corresponding principal solution exhibits the first load maximum at $\Delta/R = 0.03$ and the first global bifurcation at $\Delta/R = 0.055$. The dependence of $(\Delta_2/R)_{\min}$ on Δ/R and the dependence of $(\lambda_2/\lambda_c)_{\min}$ on Δ/R, which are depicted in Figures 5a and 5b respectively, are both monotonically increasing as for the case of the one storey shallow dome in Figures 3a and 3b. The load controlled structure is increasingly imperfection sensitive as Δ/R increases while the displacement

controlled structure is imperfection insensitive since $(\Delta_2)_{\min} > 0$ and hence all the bifurcated equilibrium paths are supercritical, *i.e.* proceed under increasing Δ.

The comparison between the exact (depicted in broken lines) and asymptotic (depicted in dotted lines) load-displacement results for all the different bifurcated equilibrium branches of this structure for two cases, one with a bifurcation point at $\Delta/R = 0.015$ and the other with a bifurcation point at $\Delta/R = 0.030$ is presented in Figure 5c. Notice the excellent agreement between exact and asymptotic solutions as well as the extreme closeness of the post-bifurcated load-displacement paths for the three different

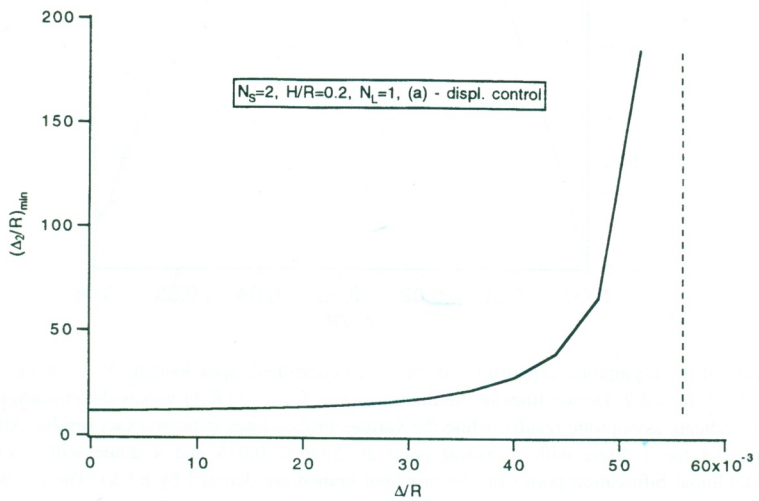

Fig. 5 a. – Imperfection sensitivity of the apex loaded $N_L = 1$ two storey shallow dome, $N_S = 2$, $H/R = 0.2$, based on the equilibrium path with the steepest load drop of the perfect structure. Graph corresponds to the displacement controlled loading and gives $(\Delta_2/R)_{\min}$ as a function of the displacement (Δ/R).

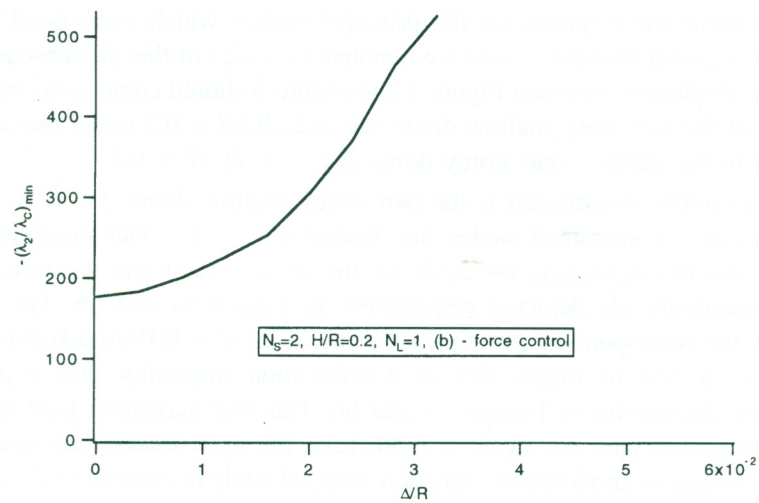

Fig. 5 b. – Imperfection sensitivity of the apex loaded $N_L = 1$ two storey shallow dome, $N_S = 2$, $H/R = 0.2$, based on the equilibrium path with the steepest load drop of the perfect structure. Graph corresponds to the force controlled loading and gives $-(\lambda_2/\lambda_c)_{\min}$ as a function of the displacement (Δ/R).

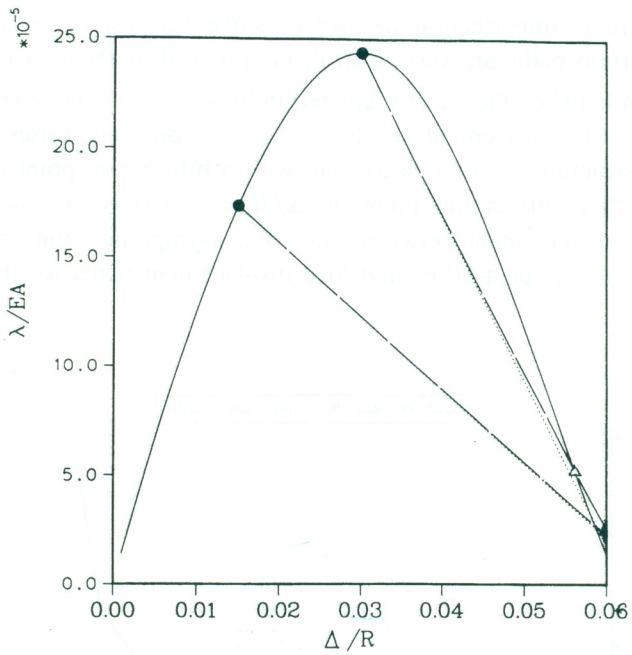

Fig. 5 c. – Validity of the asymptotic expansions for the force controlled, apex loaded, $N_L = 1$, two storey shallow dome, $N_S = 2$, $H/R = 0.2$. Dotted lines in the dimensionless force (λ/EA) versus dimensionless displacement (Δ/R) graphs indicate asymptotic results, while the various broken lines indicate exact results. All the bifurcated paths were plotted for a dome with a critical point at $\Delta/R = 0.015$ and a dome with a critical point at $\Delta/R = 0.030$. Global bifurcation points on the principal branch are denoted by a (Δ). The $(\circ)$ denotes the first instability found in the numerically calculated bifurcated equilibrium paths.

eigenmodes investigated over almost the entire range of displacements up to the first global bifurcation of the structure, marked by the first (Δ) point mark on the principal load-displacement curve (points on the principal branch which correspond to a global limit load or a global buckling mode are denoted by a (Δ) in this all subsequent similar figures). The similarities between Figure 3 and Figure 5 should come to no surprise since the top part of the two story shallow dome $N_S = 2$, $H/R = 0.2$ under one apex load is very similar to the shallow one storey dome $N_S = 1$, $H/R = 0.1$.

The final example investigated is the two storey shallow dome $N_S = 2$, $H/R = 0.2$ when all seven unconstrained nodes are loaded $(N_L = 7)$. The dependence of the $(\Delta_2/R)_{\min}$ and of $(\lambda_2/\lambda_c)_{\min}$ on Δ/R for the displacement and the force controlled loadings respectively are depicted respectively in Figures 6a and 6b. The first global instability of the corresponding principal solutions at $\Delta/R = 0.19$ (marked as previously mentioned by a $(\triangle)$ in Figure 6c), is a bifurcation instability thus explaining the corresponding asymptotes in Figures 6a and 6b. The first maximum load instability of this structure occurs later for $\Delta/R = 0.36$. Like the apex loaded one storey shallow dome $-(\lambda_2/\lambda_c)_{\min}$ is an increasing function of Δ/R while in contrast to the apex loaded shallow dome, the corresponding $(\Delta_2/R)_{\min}$ is a decreasing function of Δ/R. Notice that for $\Delta/R > 0.15$. $(\Delta_2)_{\min} < 0$, thus indicating the imperfection sensitivity of the displacement controlled structure for critical load corresponding to values $\Delta/R > 0.15$.

The comparison between the exact (depicted in several broken lines) and asymptotic (depicted in dotted lines) load-displacement results for five different bifurcated equilibrium paths for the shallow two storey dome pertaining to Figures 6a and 6b with a bifurcation point at $\Delta/R = 0.166$ is presented in Figure 6c. A magnification of the neighborhood around the bifurcation point is presented in Figure 6d. Notice the quite good agreement between exact and asymptotic results for the axisymmetric mode (the branch that emerges

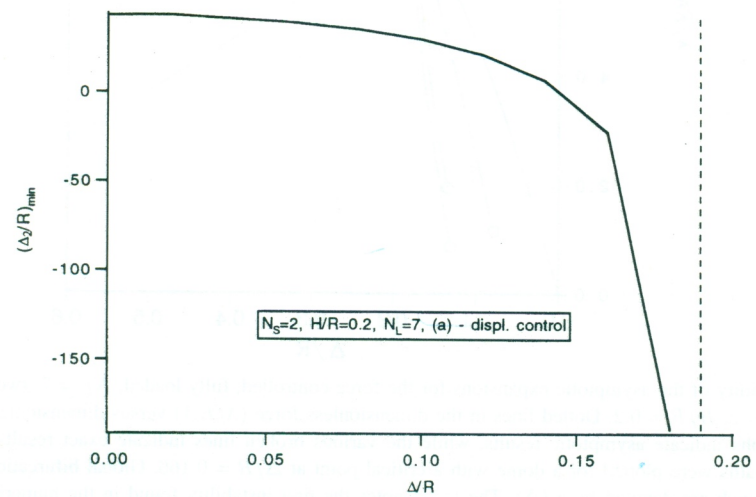

Fig. 6 a. – Imperfection sensitivity of the fully loaded $N_L = 7$ two storey shallow dome, $N_S = 2$, $H/R = 0.2$, based on the equilibrium path with the steepest load drop of the perfect structure. Graph corresponds to the displacement controlled loading and gives $(\Delta_2/R)_{\min}$ as a function of the displacement (Δ/R).

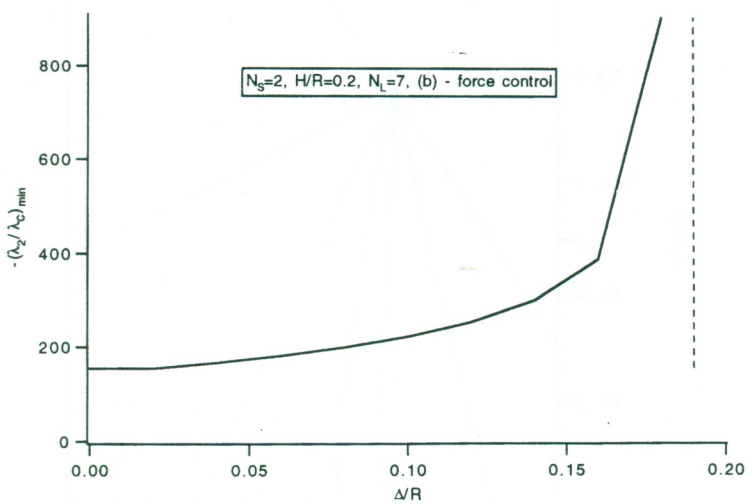

Fig. 6 b. – Imperfection sensitivity of the fully loaded $N_L = 7$ two storey shallow dome, $N_S = 2$, $H/R = 0.2$, based on the equilibrium path with the steepest load drop of the perfect structure. Graph corresponds to the force controlled loading and gives $-(\lambda_2/\lambda_c)_{\min}$ as a function of the displacement (Δ/R).

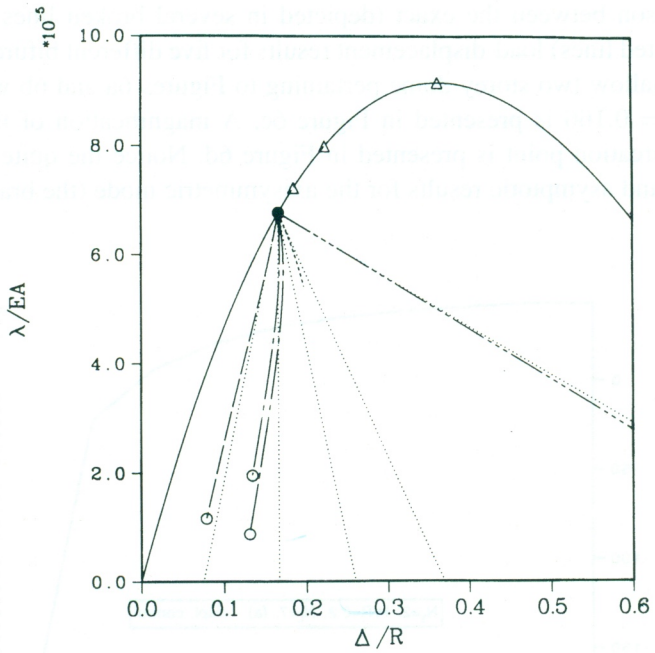

Fig. 6 c. – Validity of the asymptotic expansions for the force controlled, fully loaded, $N_L = 7$, two storey shallow dome, $N_S = 2$, $H/R = 0.2$. Dotted lines in the dimensionless force (λ/EA) versus dimensionless displacement (Δ/R) graphs indicate asymptotic results, while the various broken lines indicate exact results. Five different bifurcated paths were plotted for a dome with a critical point at $\Delta/R = 0.166$. Global bifurcation points on the principal branch are denoted by a (Δ). The $(\circ)$ denotes the first instability found in the numerically calculated bifurcated equilibrium paths.

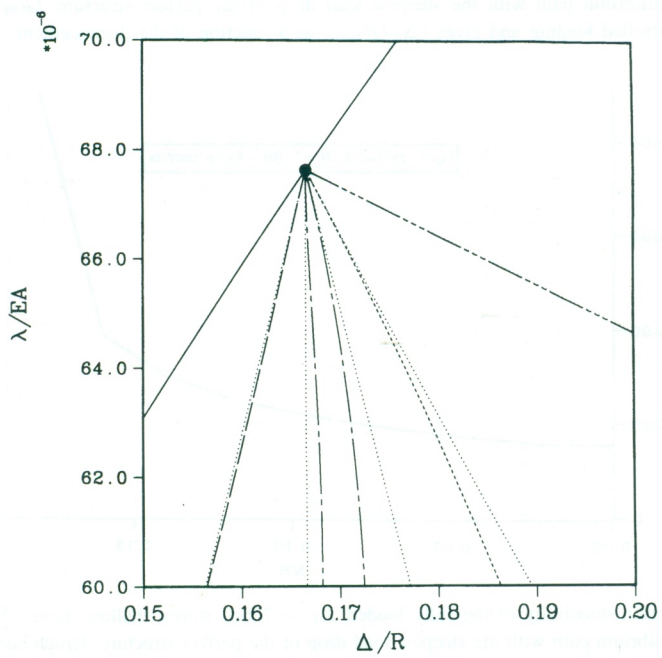

Fig. 6 d. – Magnified view of region close to the bifurcation point in Figure 6c.

almost perpendicularly from the principal solution, for which all bars in $\mathcal{G}$ buckle, *i.e.* $\mathcal{G} = \mathcal{G}_1$) and for the worst shape mode which corresponds to $(\Delta_2/R)_{\min}$ (the closest branch to the principal solution, for which only one bar buckles).

Several general remarks are in order at this point. Note that $(\Delta_2/R)_{\min}$ as well as $(\lambda_2/\lambda_c)_{\min}$ are negative for the steep one storey, apex loaded, truss and for the shallow, two storey truss loaded at all its free nodes. This property implies that neither force nor displacement control is possible for these structures beyond their first buckling load. Moreover, $(\Delta_2/R)_{\min} < 0$ implies a strong imperfection sensitivity and a snap-through buckling in either force or displacement controlled loading. Also note that, due to the strongly nonlinear principal solutions in all the truss structures investigated, there is a strong dependence of the imperfection sensitivity (as measured by $|(\lambda_2/\lambda_c)_{\min}|$ or $|(\Delta_2/R)_{\min}|$) on the prestrain of the structure. Moreover, the dependence of the imperfection sensitivity can be a non-monotonic function of the prestrain, as in the force controlled loading of the apex loaded, steep one storey dome (see *Fig.* 4b).

The final note is about the validity of the asymptotic expansions for the truss structures with out-of-straight buckling members. With the notable exception of the steep, apex loaded one storey truss, the bifurcated equilibrium paths due to the interaction of local (member buckling) modes are accurately approximated by their corresponding asymptotic expansions (see *Figs.* 3c, 5c and 6c, d). A final note should also be made about the usefulness of the asymptotic method in Section 3. Irrespective of the validity of the asymptotic results for the bifurcated equilibrium solutions, the asymptotic analysis gives the initial tangents of all these paths at critically. It is this information that we used to initiate the calculation of all the bifurcated equilibrium paths at criticality for the exact nonlinear truss model.

5. Discussion

The goal of the present paper is twofold: First, to see the effect of a strongly nonlinear prebuckling solution on the imperfection sensitivity of space trusses. Second, to assess the validity of the asymptotic expansions, used to calculate the bifurcated equilibrium paths near the critical load, by comparing them to the exact bifurcated equilibrium paths of the structure.

All the space trusses investigated have members with identical properties, *i.e.* they have the same axial and bending stiffnesses *EA* and *EI*. By varying the slenderness of the members, *i.e.* the ratio *I/A*, we can obtain a local type bifurcation mode (in which all the members with the highest axial force reach their first Euler buckling load) at any level of prestrain. Of interest is the dependence of the imperfection sensitivity of such a space structure on the slenderness ratio of the beams, or equivalently, on the level of prestrain, when the truss geometry is kept fixed. The imperfection sensitivity can be determined from the analysis of the perfect structure, by finding the bifurcated equilibrium path with the most rapid load drop, and is measured by the initial curvature of the corresponding bifurcated equilibrium path $|(\lambda_2/\lambda_c)_{\min}|$ (for force control) or $|(\Delta_2/R)_{\min}|$ (for displacement control).

Due to the strongly nonlinear principal solutions of all the truss structures investigated, we find a strong dependence of the imperfection sensitivity on the prestrain of the structure. This result is in contrast to the imperfection sensitivity results in Peek and Triantafyllidis [1992] for trusses with essentially linear principal solutions at load levels that are not in the neighborhood of a global buckling load. For all but one of the force controlled structures investigated, the imperfection sensitivity is monotonically increasing with prestrain. We also found a case (the steep one storey, apex loaded dome under force control) where the dependence of the imperfection sensitivity can be a non-monotonic function of the prestrain. In this case, the imperfection sensitivity is decreasing for higher prestrains. For several trusses, and always for adequately high levels of prestrain, we also found $(\Delta_2/R)_{\min} < 0$. This property implies that neither force nor displacement control is possible for these structures beyond their first buckling load. Moreover, $(\Delta_2/R)_{\min} < 0$ implies a strong imperfection sensitivity and a snap-through buckling in either force or displacement controlled loading.

The results concerning the validity of the asymptotic expansions for the space truss structures with out-of-straight buckling members are particularly encouraging. With the notable exception of the steep, apex loaded one storey truss, the bifurcated equilibrium paths due to the interaction of local (member buckling) modes are accurately approximated by their corresponding asymptotic expansions. It is noteworthy that for the structures which showed a good agreement between exact and asymptotic results, there was also a considerable range of validity for the asymptotic results. A final comment is in order about the asymptotic method. Irrespective of the validity of the asymptotic results for the bifurcated equilibrium solutions, the asymptotic analysis gives the initial tangents of all these paths at criticality. Hence the asymptotic analysis provides an efficient and accurate method to initiate the calculation of any bifurcated equilibrium path when the full truss model is used.

Acknowledgements

Support by N.S.F. Grant MSS-9103227 to the University of Michigan is gratefully acknowledged.

REFERENCES

ANTMAN S., 1968, General Solutions for Plane Extensible Elasticae Having Nonlinear Stress-Strain Laws, *Quart. Appl. Math.*, **26**, 35-47.

BRITVEC S. J., 1973, *The Stability of Elastic Systems*, Pergamon Press, New York, 196-248.

BRITVEC S. J., DAVISTER M. D., 1985, Post-Buckling Equilibrium of Hyperstatic Lattices, *ASCE Journal Engin. Mechanics*, **111**, 287-310.

BYSKOV E., 1979, Applicability of an Asymptotic Expansion for Elastic Buckling Problems with Mode Interaction, *AIAA Journal*, **17**, 455-459.

CASTAÑO F., 1989, *Buckling of Vierendeel Reticular Shells*, Steel Structures, Proceedings of ASCE Structures Congress, San Francisco, May 1-5.

CRAWFORD R. F., BENTON M. D., 1980, Strength of Initially Wavy Lattice Columns, *AIAA Journal*, **18**, 581-584.

ELYADA D., 1985, *Structural Analysis of Imperfect Three-Legged Truss Columns for Space Structures Applications*, Ph. D. Thesis, California Institute of Technology, Pasadena CA 91125.

KOITER W. T., 1945, *The Stability of Elastic Equilibrium*, Thesis, Technische Hooge School Delft (in Dutch). English Translation: Technical Report No. AFFDL-TR-70-25, sponsored by Lockheed Missiles and Space Co., February 1970.

KOITER W. T., 1976, *Current Trends in the Theory of Buckling,* in the Proceedings of the IUTAM Symposium on Buckling of Structures, held at Harvard University, Cambridge MA in June 1974, B. Budiansky editor, Springer Verlag, 1-16.

PEEK R., 1993, Worst Shapes of Imperfections for Space Trusses with Multiple Global and Local Modes, *Intl. J. Solids and Structures*, **30**, 2243-2260.

PEEK R., TRIANTAFYLLIDIS, 1992, Worst Shapes of Imperfections for Space Trusses with Many Simultaneous Buckling Members., *Intl. Journal Solids and Structures*, **29**, 2385-2402.

THOMPSON J. M. T., HUNT G. W., 1973, *A General Theory of Elastic Stability*, Wiley, London.

TRIANTAFYLLIDIS N., PEEK R., 1992, On the Stability and Worst Imperfection Shape in Solids with Nearly Simultaneous Eigenmodes, *Intl. Journal Solids and Structures*, **29**, 2281-2299.

WRIGHT D. T., 1965, *Membrane Forces and Buckling in Reticulated Shells*, Proc. ASCE Structural Division, **91**, 173-201.

(Manuscript received May 9, 1994;
accepted January 1, 1995.)